

Study on Seismic Performance of Autoclaved Brick Walls

Jianmin Zhang*, Zexiang Yin

Northeast Forestry University, School of Civil Engineering, Harbin 150000, China
(tumuzjm@126.com)

Abstract

In order to study the seismic performance of autoclaved brick wall, this paper conducts a low-cyclic reciprocating load test on two autoclaved brick walls with reinforced concrete columns at both ends, examines the failure characteristics, ultimate bearing capacity and deformability of the walls, and determines their hysteresis curve, skeleton curve, ductility coefficient and stiffness degradation. The results show that the wall columns exhibit good overall performance: the spacing between the columns has an obvious effect on the ductility of the walls; the smaller the spacing, the better the ductility; the column-supported walls boast excellent anti-collapse ability.

Key words

Autoclaved brick walls, Low-cyclic loading test, Bearing capacity, Deformation, Seismic behavior.

1. Introduction

Autoclaved brick is a block material made of industrial wastes (e.g. fly ash, slag) through the compression molding by large equipment, and cured by the pressure reactor at high temperature and high pressure [1]. Featuring diversified raw materials and high potential of sustainable development, it is widely regarded as an ideal wall material to replace the traditional sintered clay bricks. Previous studies have revealed that the autoclaved brick is less capable of withstanding shear force or earthquake than the ordinary clay brick, owing to the smooth surface and weak mortar adhesion. For better promotion and application of the autoclaved brick, it is imperative to improve its seismic performance [2]. As a result, this paper explores the seismic performance of

autoclaved brick wall by low cycle reciprocating test, aiming to provide reference for the popularization and application of autoclaved brick [3].

2. Specimen Design and Test Plan

2.1 Specimen Design and Fabrication

The specimens are built with MU15 autoclaved fly ash brick (240mm×115mm×53mm) and M10 special mortar [4]. The special mortar is adopted to improve the bonding effect between autoclaved brick and mortar. Two autoclaved fly ash brick walls are designed for the test, the size (height × width × thickness) of which is 1,600mm×2,000mm×240mm and 1600mm×1500mm×240mm, respectively. For each wall, both ends are installed with reinforced concrete columns (sectional size: 120mm×240mm; reinforcement: 4φ12; concrete strength grade: C30; vertical pressure: 0.6MPa) [5]. The 2,000mm-long wall is denoted as ZYGZ-01 and applied with 500mm tie bars at an interval of 500mm, while the 1,500m-long wall is denoted as ZYGZ-02 and applied with 300mm tie bars at an interval of 500mm [6]. The walls are constructed by the “one stretcher, one rowlock” method specified in the *Code for Acceptance of Constructional Quality of Masonry Structures* (GB 50203). The construction procedure is streamlined and the wall quality is better than the average. Prior to the test, the specimens have been cured for 28 days under the same conditions [7]. The specimen parameters are shown in Table 1. The vertical load distribution beam on top of each wall has a sectional size of 150mm×240mm and concrete strength grade of C30, while the grade beam has a sectional size of 350mm×300mm and the concrete strength grade of C30 [8-9].

Tab.1. Parameters of Specimens

Specimen number	Length of wall (mm)	Number of tie columns	Vertical pressure (MPa)	Actual value of strength of mortar (MPa)	Actual value of strength of bricks (MPa)
ZYGZ-01	2000	2	0.6	11.27	17.1
ZYGZ-02	1500	2	0.6	11.27	17.1

2.2 Loading Plan

The test employs the BRI-type loading device. Figures 1 and 2 illustrate the test device and the layout of the test instrument and strain gages, respectively. During the test, the vertical load is first applied to the pre-set value, and then the horizontal load is applied stage by stage in a reciprocating manner. After the wall is cracked, increase the load in each cycle by an integer

multiple of the crack displacement until the wall fails or the load drops to 85% of the ultimate load. The cracking load and cracking displacement of a specimen refer to the load and displacement when the first crack visible to the naked eyes appears on the wall. The ultimate load and ultimate displacement of the specimen stand for the maximum horizontal bearing capacity of the specimen and the corresponding displacement. The failure load and the failure displacement are measured at the moment that the horizontal bearing capacity falls to 85% of the ultimate load [10-11].



Fig.1. Picture of Loading Devices of The Test

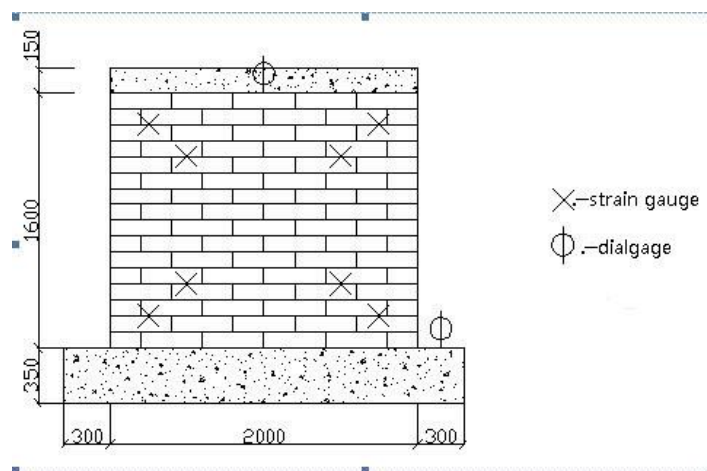


Fig.2. Floor Plan of Instrument and Strain Gauge

3. Test Results and Analysis

3.1 Specimen Failure Mode and Analysis

The two specimens, ZYGZ-01 and ZYGZ-02, share a similar failure process. Under the reciprocating load, the first oblique cracks firstly appear in the middle of the wall, and develop towards the two ends. Due to the constraint of the columns and the ring beam, the cracks are wider in the middle than in the corners. With the increase of the load, the cracks in the middle gradually

increase and widen, some bricks are crushed and exfoliated under the reciprocating action, and the columns suffer obvious bending deformation and the roughly equidistant horizontal cracks. As the loading continues, oblique cracks begin to appear in the corners of each column, which eventually cut through the column and lead to ultimate failure. Moreover, the heavily deformed bricks bulge out under the vertical stress, posing the risk of instability to the wall.

Overall, shear failure is still the dominant mode of failure in both specimens. Under heavy deformation, the columns are subjected to a certain bending deformation, and the deformation is more obvious at larger aspect ratios. The columns work synergically with the middle wall and maintain an obvious constraint effect on the latter. At the end of the test, the middle wall is severely damaged. See Figure 3 for the failure mode of the specimens.

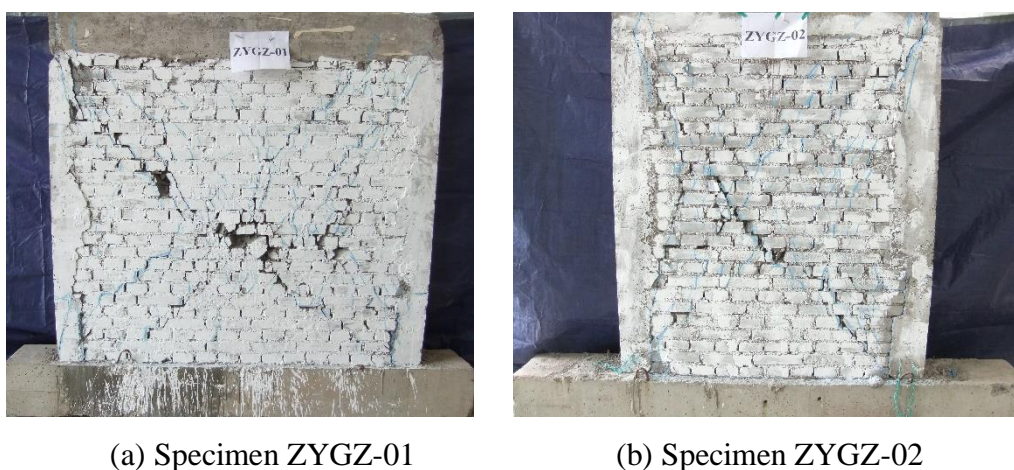


Fig.3. Failure patterns of specimens

3.2 Test Results

Table 2 shows the lateral load characteristics of the walls and the corresponding displacement values, ductility coefficients, and lateral shift angles. Specifically, the ductility coefficient refers to the ratio of the wall displacement under the ultimate load to the displacement under the cracking load, i.e. $\mu = \Delta_u / \Delta_t$; the lateral shift angle is the ratio of the wall displacement to the wall height under the failure load.

Tab.2. Results of Specimens

Specimen number	Cracking load and corresponding displacement		Ultimate load and corresponding displacement		Damage load and corresponding displacement		Ductility coefficient	Displacement
	P_t (kN)	Δ_t (mm)	P_u (kN)	Δ_u (mm)	P_f (kN)	Δ_f (mm)		

							ent $\mu=\Delta_u/\Delta_t$	angle Δ_f/h
ZYGZ-01	219	1.1	+: 279 -: 276	3.8 4.73	+: 223 -: 221	10.08 8.32	3.88	1/159
ZYPQ-02	120	0.95	+: 173 -: 156	6.82 2.73	+: 138 -: 125	16.03 12.39	5.03	1/100

The lateral load characteristics are positively correlated with the sectional area of the walls. As can be seen from Table 2, ZYGZ-01 surpasses ZYGZ-02 in terms of the cracking load, ultimate load and failure load because it has the larger sectional area between the two. With a larger spacing between the columns, ZYGZ-01 boasts smaller deformation capacity and ductility coefficient.

3.3 Functions of the Columns

With a small strain, the columns at both ends of each wall are basically in the elastic state. The rebar strain grows with the increase of the displacement. The phenomenon indicates that the columns participate in the overall work of the wall, and the participation coefficient of the columns increases with the top displacement of the wall. The effect of the columns is relatively small before the corresponding wall reaches the ultimate bearing capacity. After reaching the ultimate bearing capacity, however, the wall is held as an integral body and constrained by the columns. Despite the falling trend, the wall bearing capacity decreases rather slowly. In contrast, the columns at both ends of the wall make limited contributions to the wall bearing capacity. For each wall supported by columns at both ends, the two columns exert stronger constraint effect on the wall as they get closer to each other. Besides, the decrease in column spacing brings about apparent increase in wall ductility and much slower decrease of strength and stiffness. Figure 4 shows a typical steel strain-displacement curve.

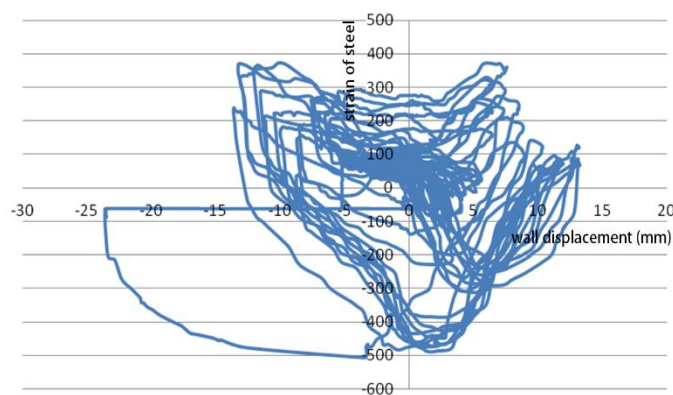


Fig.4. Strain-displacement Curve of Steel Bar in Specimens

As shown in Figure 4, the rebar is under a small strain, and the curve, as a whole, is in a “V” shape. The rebar strain peaks in the positive direction when the wall top displacement is zero, and in the negative direction when the wall top displacement reaches the maximum. With the increase of the wall top displacement, the wall becomes severely cracked and the vertical internal force is redistributed. Thus, the rebar strain continues to grow when the wall top displacement is zero. In addition, the column rebar serves as the “pin key” due to the small aspect ratio of the wall. As a result, the maximum rebar strain is positive no matter the wall top displacement reaches the positive or negative maximum.

3.4 Hysteresis Curve

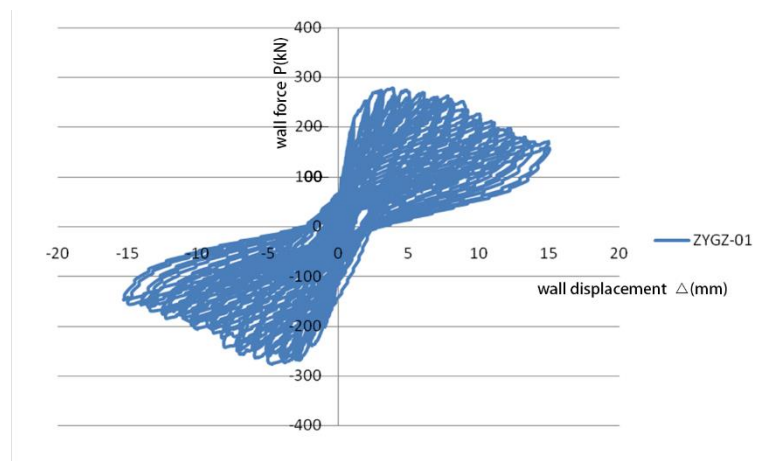


Fig.5. Hysteresis Curve of Specimen ZYGZ-01

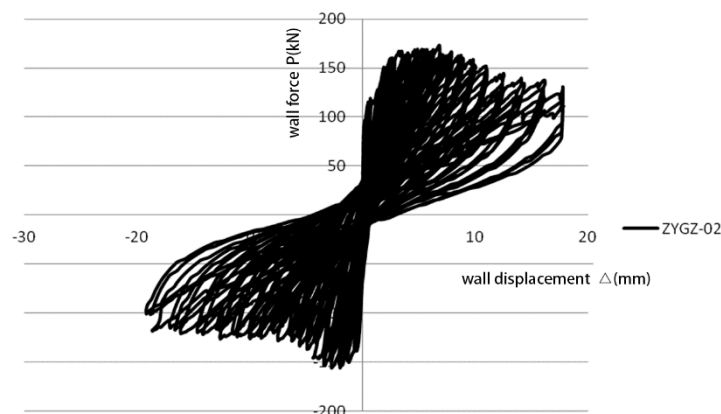


Fig.6. Hysteresis Curve of Specimen ZYGZ-02

The hysteresis curve offers a panorama of various properties of each wall under the vertical load and the horizontal reciprocating load, such as the anti-lateral displacement stiffness, the degradation of bearing capacity, ductility and the ability to dissipative seismic energy. According to the hysteresis curves of the specimens in Figures 5 and 6, the curves are basically straight under small load, indicating that the wall specimens are roughly in the elastic state with minimal top displacement and almost no residual deformation; the curves are “pinched” when cracks appear on the walls; the “pinch” phenomenon is even more obvious when the wall specimens reach the ultimate bearing capacity; in this case, the hysteresis loop is very small despite the good ductility. The wall with smaller column spacing features better deformation capacity and undergoes slower decline in strength.

3.5 Skeleton Curve

As the envelope of the hysteresis curve, the skeleton curve provides a more intuitive representation of various properties of each wall under low-cyclic reciprocating load than the hysteresis curve. The properties include the anti-lateral displacement stiffness, the degradation of bearing capacity, ductility and the ability to dissipative seismic energy, etc. Figure 7 presents the skeleton curves of the specimens. According to the figure, when the specimens are in the elastic phase, the horizontal displacement is rather limited and the skeleton curves are approximately straight; once the specimens exceed the ultimate bearing capacity, the ZYGZ-02 skeleton curve descends slower than that of ZYGZ-01.

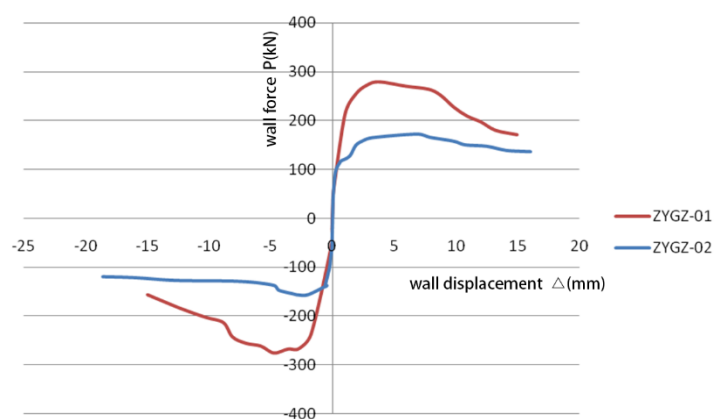


Fig.7. Skeleton Curve of Specimen

3.6 Stiffness Degradation Curve

The equivalent stiffness of each wall K_i is the secant stiffness of the vertex in each cycle, i.e.:

$$K_i = \frac{|P_i| + |-P_i|}{|\Delta_i| + |-\Delta_i|} \quad (1)$$

Where P_i is the horizontal load in the i -th cycle; $-P_i$ is the reverse horizontal load; Δ_i is the displacement corresponding to P_i ; $-\Delta_i$ is the displacement corresponding to $-P_i$.

The equivalent stiffness of each wall is obtained by formula (1), and the corresponding stiffness degradation curve is shown in Figure 8. It can be seen from the figure that curves of the two walls are basically in the same shape. In spite of the large initial stiffness difference, there is no significant stiffness difference after cracking.

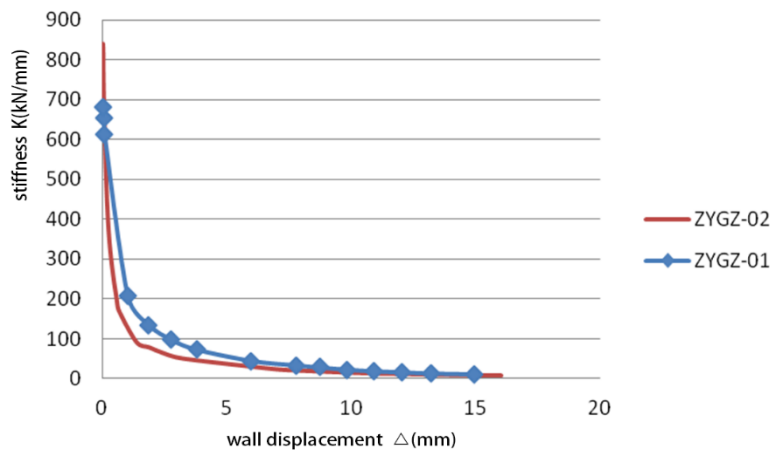


Fig.8. Stiffness Degradation Curves of Specimen

Conclusion

Through the experiment on two specimens of autoclaved fly ash brick walls under low cyclic reciprocating load, this paper probes into the failure characteristics, ultimate bearing capacity and deformation capacity of the walls, and determines their hysteresis curve, skeleton curve, ductility coefficient and stiffness degradation. The main conclusions are as follows:

(1) The application of reinforced concrete columns maintains the integrity of the wall after cracking; the columns at the two ends have obvious constraining effect; the wall supported by the two end columns features good anti-collapse ability.

(2) The wall supported by the two end columns has an obviously “pinched” hysteresis curve, strong deformation capacity, and weak energy dissipation ability.

(3) The column spacing has limited influence on the wall bearing capacity, which is determined by the length of the wall. However, the spacing has a direct bearing on the ductility and deformation capacity. Smaller spacing contribute to better ductility of the wall.

References

1. D.X. Tang, masonry structure, 2003, Beijing: Higher Education Press (HEP).
2. H.D. Huang, J. Yuan, Present situation, problems and solutions of autoclaved brick development in China, 2009, *New Building Materials*, no. 12, pp. 47-48.
3. F.L. Wang, Y.L. Gao, H. Zhang, Application of new masonry structure system and wall material engineering, 2010, China Building Material Industry Press.
4. C.W. Zhao, H. Qiao, L.Y. Gao, Experimental Study on Seismic Behavior of Autoclaved Fly Ash Solid Brick Walls, 2010, *Journal of Shenyang Jianzhu University Natural Science*, vol. 26, no. 3, pp. 439-445.
5. L. Fang, J.G. Liang, An experimental study on seismic performance of autoclaved fly ash wall bricks, 2008, *Journal of Hunan Agricultural University (Natural Sciences)*, vol. 34, no. 2, pp. 240-244
6. GB50011-2010 Code for Seismic Design of Buildings, Beijing: China Architecture & Building Press, 2010.
7. GB50203-2011 Code for Acceptance of Constructional Quality of Masonry Structures, 2011, Beijing: China Architecture & Building Press.
8. F. Li, Earthquake-Resistance Performance Researching of Brick Wall with Structure Column, Ring Girder and Horizontal Ribs, 2004, Xian University of Architecture and Technology.
9. GB50003—2011 Code for Design of Masonry Structures, 2011, Beijing: China Architecture & Building Press.
10. B.Z. Zhou, J.Q. Xia, Experimental study on seismic behaviour of brick masonry with horizontal reinforcement, 1991, *Journal of Building Structures*, vol. 12, no. 4, pp. 31-43.
11. Z.G. Wang, G.Y. Xue, B.L. Gao, J.T. Zhang, Experimental research on the seismic behavior of confined shale brick masonry walls, 2003, *Journal of Southeast University*, vol. 33, no. 5, pp. 638-648.